Article

Surface Confined Metallosupramolecular Architectures: Formation and Scanning Tunneling Microscopy Characterization

Shan-Shan Li, Brian H. Northrop, Qun-Hui Yuan, Li-Jun Wan, and Peter J. Stang

Acc. Chem. Res., **2009**, 42 (2), 249-259• DOI: 10.1021/ar800117j • Publication Date (Web): 15 December 2008

ACCOUNTS
of chemical research

Surface Confined Metallosupramolecular Architectures: Formation and Scanning Tunneling Microscopy Characterization

SHAN-SHAN LI,[†] BRIAN H. NORTHROP,[‡] QUN-HUI YUAN,[†] LI-JUN WAN,[†,*] AND PETER J. STANG[‡,*]

[†]*Beijing National Laboratory for Molecular Sciences, Institute of Chemistry, Chinese Academy of Sciences, Beijing 100190, China,* [‡]*Department of Chemistry, University of Utah, 315 South 1400 East, Salt Lake City, Utah 84112*

RECEIVED ON MAY 21, 2008

CONSPECTUS

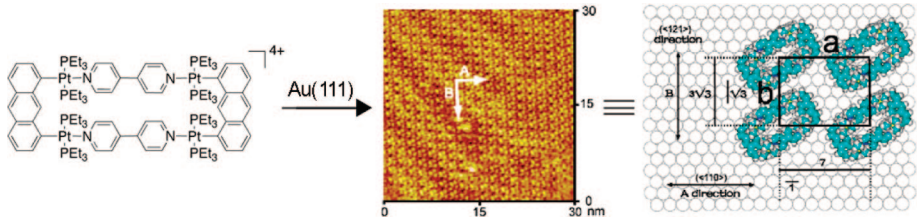

Metallosupramolecular compounds have attracted a great deal of attention over the past two decades largely because of their unique, highly complex structural characteristics and their potential electronic, magnetic, optical, and catalytic properties. These molecules can be prepared with relative ease using coordination-driven self-assembly techniques. In particular, the use of electron-poor square-planar Pt(II) transition metals in conjunction with rigid, electron-rich pyridyl donors has enabled the spontaneous self-assembly of a rich library of 2D metallacyclic and 3D metallacage assemblies via the directional-bonding approach. With this progress in the preparation and characterization of metallosupramolecules, researchers have now turned their attention toward fully exploring and developing their materials properties.

Assembling metallosupramolecular compounds on solid supports represents a vitally important step toward developing their materials properties. Surfaces provide a means of uniformly aligning and orienting these highly symmetric metallacycles and metallacages. This uniformity increases the level of coherence between molecules above that which can be achieved in the solution phase and provides a way to integrate adsorbed layers, or adlayers, into a solid-state materials setting. The dynamic nature of kinetically labile Pt(II)−N coordination bonds requires us to adjust deposition and imaging conditions to retain the assemblies' stability. Toward these aims, we have used scanning tunneling microscopy (STM) to image these adlayers and to understand the factors that govern surface self-assembly and the interactions that influence their structure and stability.

This Account describes our efforts to deposit 2D rectangular and square metallacycles and 3D trigonal bipyramidal and chiral trigonal prism metallacages on highly oriented pyrolytic graphite (HOPG) and Au(111) substrates to give intact assemblies and ordered adlayers. We have investigated the effects of varying the size, symmetry, and dimensionality of supramolecular adsorbates, the choice of substrate, the use of a molecular template, and the effects of chirality. Our systematic investigations provide insights into the various adsorbate−adsorbate and substrate−adsorbate interactions that largely determine the architecture of each assembly and affect their performance in a materials setting. Rational control over adlayer formation and structure will greatly enhance the potential of these supramolecules to be used in a variety of applications such as host−guest sensing/diagnostic systems, molecular electronic devices, and heterogeneous stereoselective synthesis and catalysis.

Introduction

In recent years, considerable attention has been paid to the design and synthesis of molecular materials and devices.[1] As a result, a host of fascinating molecules have been developed that exhibit desirable electronic, magnetic, photonic, mechanical, and sensing/diagnostic properties,[1,2] giving rise to the nascent field of molecular nano-

Published on the Web 12/15/2008 www.pubs.acs.org/acr
10.1021/ar800117j CCC: $71.50

technology. The properties of most examples of molecular materials have been investigated through solution phase studies. While the solution phase lends itself to a wide variety of analytical techniques, it is, perhaps, not the most beneficial environment for the operation of advanced materials because it generally lacks coherence, prohibiting large-scale uniformity and coordination in the operations of functional materials. Assembling molecules on surfaces, however, imparts a very high degree of coherence in their orientation, alignment, and packing provided that well-defined, uniform adlayers of the absorbates can be obtained.[3] Furthermore, solid surfaces provide a means of integrating molecular adlayers with well-known and thoroughly studied material substrates (e.g., SiO_2, gold, ITO, HOPG, etc.) in a conventional device setting.[4] To fully take advantage of the benefits of surface adsorbed molecular materials, it is necessary to obtain a high level of understanding of the factors that govern and control the assembly of uniform, ordered adlayers.

A number of powerful top-down fabrication techniques have been developed, particularly by Whitesides[5] and others,[6] for the creation of patterned molecular monolayers. Electron-beam, soft, and photolithography allow for intricately designed surfaces to be tailored for specific applications. Most top-down techniques, however, have limitations[5] below 50−100 nm^2. As an alternative to top-down protocols, bottom-up strategies[7] have been developed for the preparation of molecular films and self-assembled monolayers (SAMs). In this regard, molecular self-assembly and self-organization have attracted considerable attention.

Self-assembly is a natural and spontaneous process that is of ever increasing importance in chemistry and materials science.[8−10] Molecular self-assembly relies upon the various strengths of noncovalent interactions to bring together predesigned building components to construct complex supramolecules similar to how the same process is done throughout nature.[11] The use of noncovalent interactions allows the assembly process to be thermodynamically controlled, most often resulting in the formation of a single, discrete supramolecule. In this regard, self-assembly is able to quite literally build complex molecules from the bottom-up and is an increasingly used strategy for nanofabrication, which is a promising supplement to microfabrication techniques.[12−15]

Over the past two decades, many metal−ligand coordination-based motifs for the self-assembly of metallosupramolecules have been developed and explored.[16−21] These metallosupramolecules possess ample functionality such as catalytic, photophysical, electronic, or redox properties[22] and are ideal building blocks for sensors,[23] information storage materials,[24] and nanodevices.[25] In particular, by combining rigid, electron-poor metal acceptors, such as square-planar Pt(II) metal centers, and rigid, electron-rich organic donors, often pyridyl- or nitryl-containing molecules, we have systematized the "directional-bonding" approach[16] to coordination-driven self-assembly. Carefully designing component building units allows for a variety of two-dimensional (2D) metallacycles[16b,c] and three-dimensional (3D) metallacages[16a,b] to be prepared under mild reaction conditions in high isolated yields (typically >95%). These supramolecules have been extensively studied in the solution phase and in the solid state. Much less is known, however, about their conformations and behavior on solid surfaces. Understanding the formation of stable metallosupramolecular adlayers is a significant fundamental step toward the fabrication of nanostructures and nanodevices and requires a powerful means of fully characterizing such surfaces. Scanning probe microscopies, in particular scanning tunneling microscopy (STM) and electrochemical STM (ECSTM), have proven to be powerful tools for studying surface adlayers.[26−30] STM has unparalleled high and spatial resolution and is able to provide real-time, real-space 3D structural information of surfaces up to atomic resolution. High-resolution images provided by STM can be used to determine the stability of adlayers as well as the structural details of adsorbed molecules such as their orientation, alignment, and nearest neighbor proximity. STM also provides a means for determining how small changes in the chemical structure of adsorbates translate into changes in the adsorption, mobility, lateral interactions, and architecture of the resulting molecular adlayer.

To date, numerous organic, inorganic, and biological molecules have been assembled on solid surfaces under ultrahigh vacuum (UHV), ambient, and solution deposition conditions.[3] There have been few literature reports,[31−34] however, on the adsorption of metal-coordinated metallosupramolecules on surfaces. Schalley and co-workers, for example, have successfully templated adlayers of supramolecular squares[34a] and chiral rhomboids[34b] on Cl^--modified Cu(100) surfaces and demonstrated that a combination of adsorbate−substrate Coulombic and adsorbate−adsorbate van der Waals interactions governed the adlayer conformation.

Over the past few years, we have successfully prepared multiple well-defined adlayers of metallosupramolecular assemblies on solid surfaces and have characterized their conformations using STM.[35−38] A variety of large, complex coordination compounds, differing in their size, geometry, dimensionality, and chirality, have been utilized in the formation of monodisperse adlayers. These surface-confined supramolecules represent an impressive display of higher-or-

SCHEME 1. Schematic Representation of the Three Techniques Used in the Self-Assembly of Metallosupramolecular Adlayers on HOPG and Au(111) substrates[a]

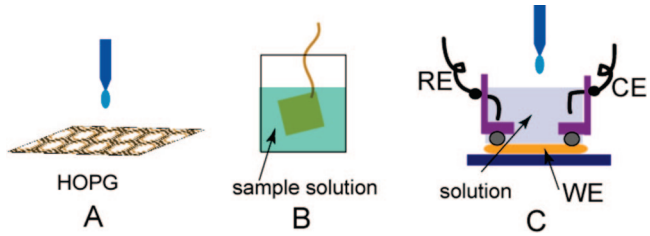

[a] (A) Solution deposition; (B) substrate immersion; (C) aqueous *in situ* adsorption. RE = reference electrode; CE = count electrode; WE = working electrode.

der assembly wherein both the metal−organic supramolecules and the adlayers themselves are formed by spontaneous self-assembly under mild conditions. This Account summarizes our recent successes in the formation and characterization of metallosupramolecules on solid surfaces.

Formation of Self-Assembled Architectures on Solid Surfaces

Molecules and supramolecules can be assembled onto surfaces by a variety of methods.[3,5,6,12−15,39] Common among them are ultrahigh vacuum (UHV),[3] solution deposition/immersion,[39] and Langmuir−Blodgett.[40] The dynamic nature[20] of metal−organic dative bonds in most supramolecular coordination assemblies, however, can complicate the adlayer formation process. For example, evaporation techniques under UHV require heating samples at high temperatures that induce dissociation of coordination bonds. Furthermore, it has been observed[41] that dissociation can occur during solution phase assembly because competitive equilibria may exist between the metal substrates and the kinetically labile coordination bonds in the metal−organic supramolecules. It is possible, however, to form well-defined adlayers of supramolecular architecures on surfaces such as Au(111) and highly oriented pyrolytic graphite (HOPG) under mild conditions at ambient temperatures and in an electrolyte solution.

The three solution phase methods we have used in the formation of adlayers of metallosupramolecular assemblies are shown in Scheme 1. Solution deposition is used for the preparation of adlayers on HOPG (Scheme 1A) whereby a drop of solution containing the desired molecule(s) is deposited on an atomically flat surface of freshly cleaved HOPG. The adlayer is observed following evaporation of the solvent. The formation of supramolecules on metallic crystals such as Au(111) involves immersion of the metallic solid in a solution containing the metallosupramolecule(s) for a period of several seconds to minutes (Scheme 1B). The solution can be organic (e.g., ethanol or toluene) or aqueous electrolyte depending on which environment allows the adsorbate to retain its chemical structure without dissociation. For metallosupramolecules that are soluble in H_2O, an aqueous solution of the adsorbate can be prepared and directly added to an electrochemical cell in an electrochemical STM (Scheme 1C). The use of metals such as Au(111) in an electrochemical environment requires that the electrode potential applied to the substrate be controlled at the double layer region where no redox reaction(s) can occur.

Adlayers of 2D Metallosupramolecules on Au(111)

Metallosupramolecules exhibit ample functionality with a high degree of symmetry as well as unique morphologies[16−21,42,43] and are promising candidates for materials applications. Their potential uses may be better exploited when incorporated onto solid surfaces where their high symmetry can allow for the formation of precisely aligned, uniform adlayers and lead to enhanced coherence and potential amplification of their desirable materials properties.[44] Prior to fabricating metallosupramolecule-based hybrid devices, however, it is necessary to gain an understanding of the conformations adopted by adsorbates on different surfaces. Toward this aim, adlayers of three 2D supramolecular metallacycles, two rectangles[45] and one square[46] (Figure 1), have been formed on Au(111) surfaces and are imaged by ECSTM. Though the structures of the two supramolecular rectangles are quite similar and largely symmetric, they do differ significantly in the length of their long edges: 2.1 nm for **1** and 3.1 nm for **2**. Insight into the effects of size can be gathered through comparisons of these two rectangular supramolecules. The structure of supramolecular square **3** is slightly more complex. The X-ray suprastructure of the square shows that two sets of PPh_2 ligands point inward along one diagonal, while along the other diagonal they point outward, allowing for the effects of this decrease in symmetry to be examined.

Figure 2A is a typical STM image of the adlayer formed by small rectangle **1** on a Au(111) surface.[35] A highly ordered adlayer of the rectangle extends as a single domain across the atomically flat terrace of the Au(111) surface. Rows of rectangles extend along the *A* and *B* directions and cross each other at an angle of 90° ± 2°. In the high-resolution STM image (Figure 2B), each supramolecular rectangle appears as a set of four bright spots, highlighted by white ovals, corresponding to the anthracene and bipyridyl moieties of **1**. The dimensions of each supramolecular rectangle are 2.0 nm × 1.2 nm, consistent with the size of the rectangle previously determined from X-ray crystallography.[45] Packing of rows along the *B* direction of the adlayer closely resembles their arrangement within the *a*−*c* plane of the crystal of **1**. In the 3D crystal,

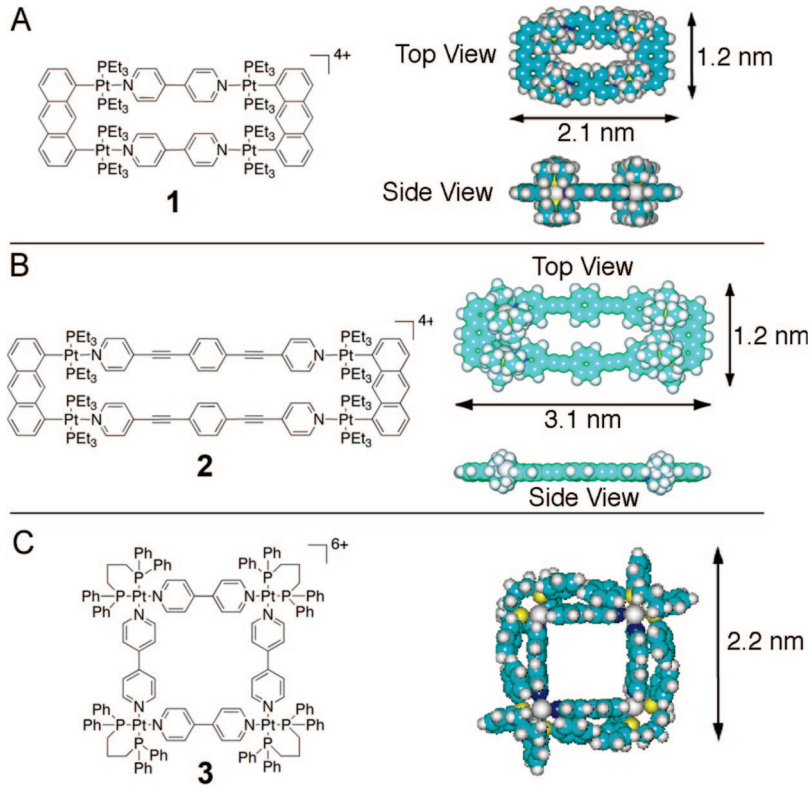

FIGURE 1. Chemical structures and space-filling models of (A) "small" supramolecular rectangle **1**, (B) "large" supramolecular rectangle **2**, and (C) supramolecular square **3**.

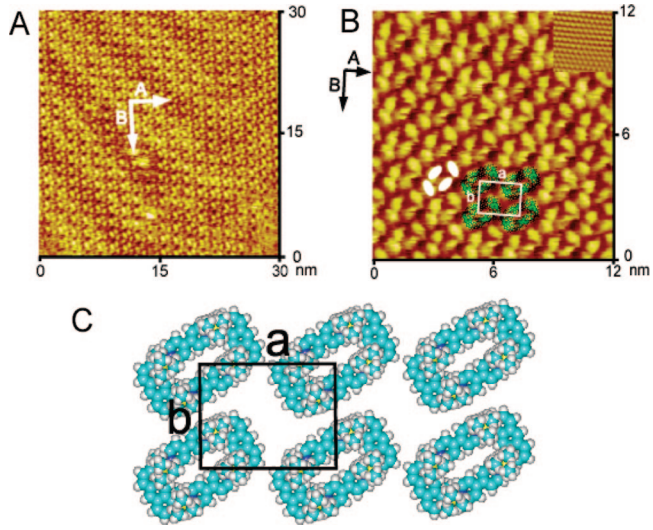

FIGURE 2. (A) Large-scale and (B) high-resolution STM images showing the face down orientation of the adlayer of rectangle **1** on Au(111) and (C) unit cell and proposed structural model of the adlayer.

however, adjacent rows in the *a*−*c* plane are packed more tightly than they are in the 2D adlayer. Each molecule preserves its rectangular shape with a dark depression in the center (Figure 2B). The intermolecular distance and molecular conformation demonstrate a flat-lying orientation of the supramolecular rectangle on the Au(111) surface. This orientation, with the plane of both the anthracene and bipyridyl aromatic moieties oriented parallel to the Au(111) surface, maximizes favorable Au−π interactions, while weaker van der Waals forces govern the long-range lateral ordering of the adlayer. A unit cell is described in Figure 2B, and a structural model for the adlayer is proposed in Figure 2C.

The large-scale STM image shown in Figure 3A reveals the well-ordered adlayer of the large supramolecular rectangle **2** on Au(111).[36] The structural details of the adlayer are shown in the high-resolution STM image (Figure 3B). Bright rows of rectangles are observed along direction *A*, adopting a similar planar orientation as they do along the *b*−*c* diagonal in the solid state. Separate individual molecules could be found on the Au(111) surface and were used to image an individual rectangle, as shown in the high-resolution STM image in the upper right corner of Figure 3B. The molecule appears to contain two dark depressions, which correspond to the space between the bis-Pt(II) anthracene acceptors and the phenylene units of the linear 1,4-bis(4-ethynylpyridyl)phenyl donors. The dimensions of each molecule were measured at 3.0 nm × 1.1 nm, consistent with the size of the rectangle determined from X-ray crystallography.[45] A unit cell is shown in the high-resolution figure. These details demonstrate a flat lying orientation of the rectangle on the Au(111) surface, preserving its rectangular shape and, as with

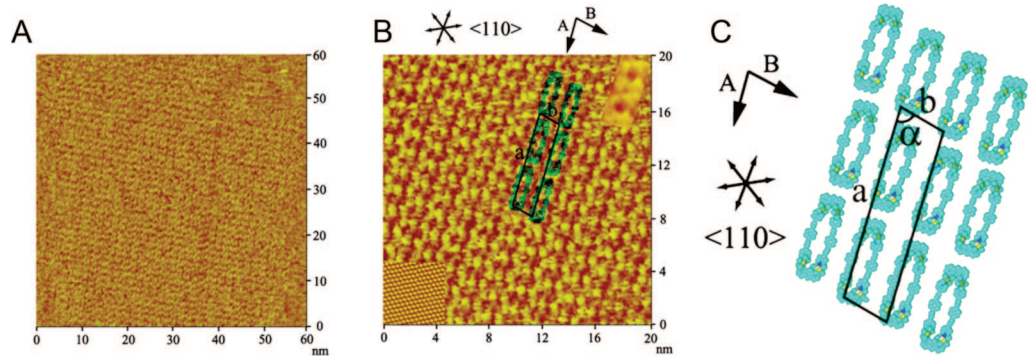

FIGURE 3. (A) Large-scale and (B) high-resolution STM images showing the face down orientation of rectangle **2** on Au(111) and (C) unit cell and proposed structural model of the adlayer.

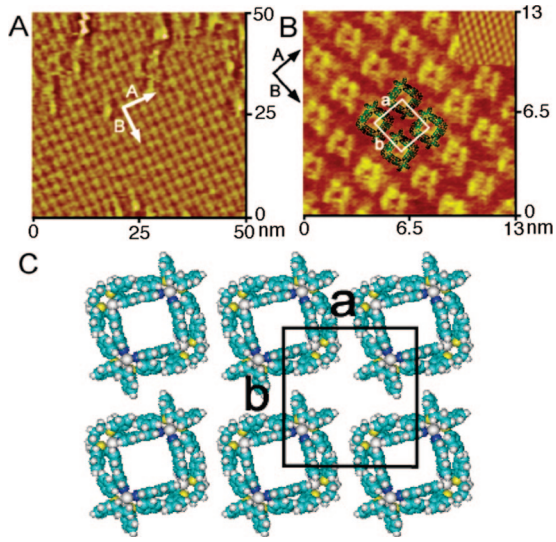

FIGURE 4. (A) Large-scale and (B) high-resolution STM images of the adlayer of square **3** on Au(111) and (C) unit cell and proposed structural model of the adlayer.

rectangle **1**, maximizing Au−π interactions. A structural model is proposed in Figure 3C. It is interesting to note that adjacent rows of the smaller supramolecular rectangle **1** form a more staggered adlayer on Au(111) than do adjacent rows of the larger supramolecular rectangle **2**. This subtle change in the lateral ordering and difference in adlayer orientation likely results from increased intermolecular van der Waals interactions between the long edges of rectangle **2** compared with the shorter edges of rectangle **1**.

Figure 4A shows a large-scale STM image of the supramolecular square (**3**) adsorbed on a Au(111) surface.[35] While the adlayer consists of regular rows of square **3** extending in the *A* and *B* directions and forming an angle of 90°, the adlayer does not extend as far as adlayers of rectangles **1** and **2**, reflecting a difference in adlayer stability likely caused by the lower symmetry of supramolecular square **3**. The structural details are seen in the high-resolution STM image (Figure 4B). Each molecule appears as a square with a dark depression in the center. The molecular size of the square is determined to be 2.1 ± 0.1 nm on each side, consistent with crystal parameters.[46] The PPh_2 groups can be clearly distinguished in the high-resolution image. None of the four sides of the square are flat, owing to the different orientations of the PPh_2 ligands of **3**. Therefore, the metallacycles adopt a face-down orientation with their interior cavities oriented parallel to the substrate. The crystal structure of square **3** reveals that the supramolecules stack into channels along the *b*-axis while along the *a*- and *c*-axes they align into regular rows similar to their adlayer structure, though neighboring molecules pack more closely in the crystal. It is believed that, in the absence of Au−π contacts, adlayer stability and ordering is achieved primarily through weaker intermolecular van der Waals interactions, possibly contributing to the difference in adlayer stability. A unit cell is superimposed on the STM image of Figure 4B, and a schematic model for the supramolecular adlayer on a Au(111) surface is proposed in Figure 4C. The observations gathered by studies of 2D rectangular and square metallacycles on Au(111) lend considerable insight into the effects of size and symmetry on the formation of adlayers of self-assembled metallosupramolecules.

Substrate Effects on Metallosupramolecular Adlayers

It is well-known that the adsorption of single organic molecules on solid surfaces is primarily governed by intermolecular and molecule−substrate interactions and that every stable adlayer reflects a thermodynamic minimum that maximizes the contributions of these interactions.[3] To date, however, there are few studies investigating the effects of substrate on metal−organic coordination compounds. In order to investigate the effects of different solid supports on adlayer conformations, we investigated adlayers of the large supramolecular rectangle **2** on HOPG and have resolved their packing arrangement and internal molecular structure.[36]

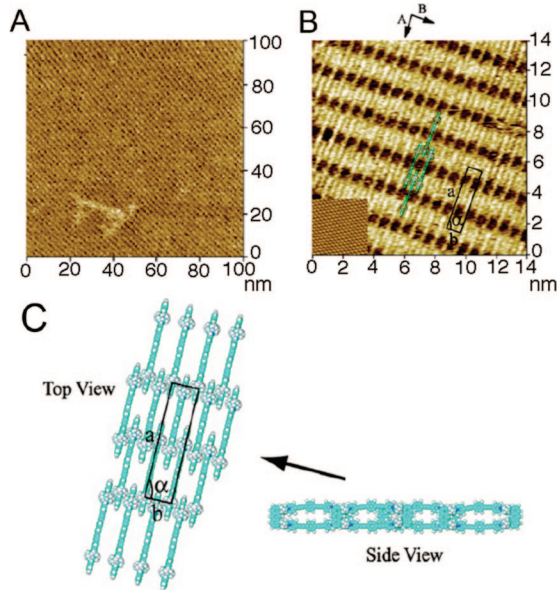

FIGURE 5. (A) Large-scale and (C) high-resolution STM images showing an edge down orientation of the adlayer of rectangle **2** on HOPG and (C) proposed structural model.

Adlayers of the supramolecular rectangle were prepared by depositing a drop of **2** (10^{-6} M in toluene) onto a freshly cleaved HOPG surface. Figure 5A is a large-scale STM image of **2** adsorbed onto HOPG.[36] The molecules organize into a well-ordered two-dimensional array with regular molecular rows. Careful examination of the high-resolution STM image (Figure 5B) shows that the prominent components of the molecular adlayer are rows of bright lines. The lines are observed to extend along the *A* direction with a length of 3.1 $\pm$ 0.1 nm, while along the *B* direction the neighboring lines are interdigitated and form a close-packed arrangement. When viewed along the *B* direction, the distance between two bright lines is 1.2 $\pm$ 0.1 nm. The length of these lines along the *A* direction is consistent with the dimensions of the long side of the supramolecular rectangles.[45] These results indicate that each bright line corresponds to a single rectangle and that the rectangles stand vertically with their long edges perpendicular to the plane of the HOPG surface, similar to their crystal packing along the *a*-axis of the crystal. A proposed model of the supramolecular rectangular structure is shown in Figure 5C, as is a unit cell.

The observation that supramolecular rectangle **2** adopts two completely different orientations on Au(111) (Figure 3) and HOPG (Figure 5) surfaces demonstrates that adlayers of self-assembled metal-coordinated supramolecular architectures can be dominated by solid supports. Substrate–adsorbate interactions are weaker between rectangle **2** and HOPG than they are between **2** and Au(111), presumably due to the strong Au–π interactions that are maximized when the supramolecular rectangles lay flat with their aromatic planes parallel to the surface. Self-assembly on the HOPG surface, on the other hand, is primarily governed by intermolecular $\pi-\pi$ and van der Waals interactions between adjacent rectangles, causing the rectangles to adopt a close-packed 2D molecular network with a vertical orientation of the molecules.

In light of the differences observed between adlayers of the supramolecular rectangle **2** on Au(111) and HOPG surfaces, the conformation of the smaller supramolecular rectangle **1** was also investigated on HOPG. However, all attempts to form well-ordered adlayers of **1** on HOPG were unsuccessful, highlighting the effects that size and the choice of substrate can have on adlayer formation. The formation of well-defined adlayers of the supramolecular rectangle **1** is likely hindered by its smaller size (2.1 nm $\times$ 1.2 nm) compared with rectangle **2** (3.1 nm $\times$ 1.2 nm). Given that intermolecular forces are the primary driving force for the formation of such adlayers on HOPG, the decreased surface area of rectangle **1** subsequently decreases the extent to which intermolecular $\pi-\pi$ and van der Waals interactions can help stabilize a self-assembled adlayer, prohibiting adlayer formation.

Control of Adlayer Formation with a Molecular Template

With the goal of fabricating functional materials in accordance with the "bottom-up" strategy of materials science and molecular nanotechnology comes the necessity to be able to rationally design and control molecular structures at the nanoscale. Therefore, in an effort to tune the self-assembly of the small supramolecular rectangle **1** from a disordered adlayer on HOPG to an ordered one, a molecular template has been employed.[37] With this strategy, the disordered molecular architecture previously observed on HOPG is regulated into an ordered adlayer with monodispersion.

The choice of template is critical when attempting to achieve a templated self-assembly of any molecule on a solid substrate. Many interactions (template–template, adsorbate–template, template–surface, and adsorbate–surface) contribute to the success or failure of templated assembly. These interactions, along with appropriate size complementarities, constitute the major driving forces for templation and monodispersion. In the case of templating supramolecular rectangle **1** on HOPG, a triple-armed amphiphile, 1,3,5-tris(10-carboxydecyloxy)-benzene (TCDB), was selected. The structural details of the TCDB template on HOPG are revealed in the high-resolution STM image (Figure 6A).[37] The bright spots in the image correspond to the TCDB benzene core, and the chains are the carboxydecyloxy "arms".[47] An important structural feature in the image is the existence of quasi-rectan-

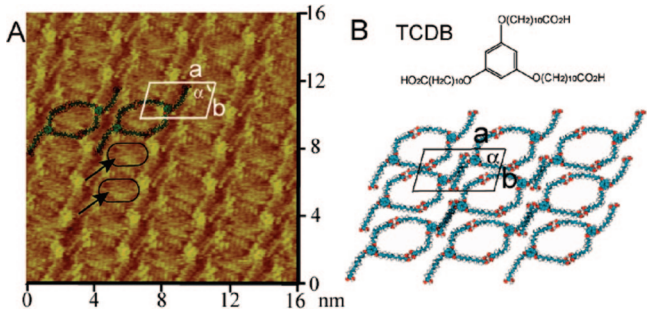

FIGURE 6. (A) High-resolution STM images of the TCDB molecules adsorbed on HOPG. Unfilled ovals indicated by arrows highlight the existence of voids in the adlayer. (B) Chemical structure of TCDB as well as proposed structural model and unit cell of its adlayer on HOPG.

gular cavities, as indicated by unfilled ovals. The carboxy functionalities of adjacent arms strive to maximize the number of strong hydrogen-boding interactions, thus leaving regular, well-formed tetragonal voids between the stretched out arms of TCDB within the adlayer whereas related triply symmetric benzoic acid templates typically form hexagonal honeycomb networks.[48] As measured with STM, the size of each cavity is 2.4 nm × 1.3 nm (±0.2 nm). A unit cell for the adlayer is outlined in Figure 6A. Figure 6B is a proposed structural model of the hydrogen bound, self-assembled 2D network. TCDB was chosen as a potential template for **1** given the high degree of complementarity between the dimensions of the cavity formed in the TCDB adlayer and those of supramolecular rectangle **1**: 2.1 nm × 1.2 nm.

To test the ability of TCDB to act as a template for **1**, an ethanolic solution ($<10^{-4}$ M) containing a TCDB/rectangle mixture (1:3) was deposited on a HOPG surface. With the assistance of the TCDB molecular template, the disordered adlayer previously observed upon deposition of supramolecular rectangle **1** on HOPG was successfully regulated into an ordered self-assembly with monodispersion.[37] Figure 7A is a large-scale STM image of the mixed adlayer. Dashed lines indicate the existence of several domains, each with extending molecular rows. Similar molecular arrangements exist in each domain. As seen in both the large-scale (Figure 7A) and high-resolution (Figure 7B) images, the adlayer differs from both the pure, ordered TCDB adlayer and the pure, disordered rectangle adlayer. The most noticeable difference is the appearance of well-dispersed bright ovals. Throughout the adlayer, these bright ovals are positioned where the dark vacancies in the pure TCDB adlayer had been, indicating that the supramolecular rectangles have become entrapped in the molecular template forming an ordered assembly. The dimensions of the bright ovals are 2.1 nm × 1.2 nm, which match those of the supramolecular rectangle. A unit cell for the structure is outlined in Figure 7B, and a structural model is proposed in Figure 7C. Unit cell parameters of *a* and *b* closely resemble those of the TCDB networks in Figure 6A, although the unit cell angle α is increased from 75° to 90°.

The successful self-assembly of the supramolecular rectangles on a HOPG surface is achieved because of intermolecular template−rectangle interactions and the complementarity between the structural parameters of the TCDB adlayer and **1**. It is striking that the supramolecular rectangles lay "flat" on the HOPG surface, analogous to their conformation[35] on Au(111) (Figure 2) as opposed to lying perpendicular[36] to the HOPG surface as do the related, larger supramolecular rectangles **2** (Figure 5). The length of and intermolecular hydrogen bonding between the alkyl chains of TCDB determine the size and shape of adlayer cavities, which can promote the entrapment of appropriately sized molecules[47] or supramolecules[37] through stabilizing van der Waals interacions. The flexibility of the alkyl chains enables the TCDB template to undergo minor structural changes in order to accommodate guests without disrupting the underlying stability of the template adlayer. For example, the unit cell parameter α changes from a slightly rhomboidal 75° in the pure TCDB adlayer to a rectangular 90° in the mixed adlayer to accommodate the entrapped rectangles and maximize the stabilizing van der Waals interactions. Altogether, the combination of geometric parameters and intermolecular TCDB−**1** and TCDB−HOPG interactions promote the template-directed self-assembly and monodispersion of supramolecular rectangles **1** on an HOPG surface, thus demonstrating a highly desirable degree of control over adlayer formation.

Adlayers of 3D Metallacages on Au(111)

In addition to 2D metallacyclic supramolecules, 3D metallacages have also been shown to form ordered adlayers on Au(111).[35,38] The assembly of 3D supramolecules on surfaces presents a more complex situation than 2D assemblies given the more complex shapes that can be formed in three dimensions. The D_{3h}-symmetric trigonal bipyramid,[49] TBP (Figure 8A), for example, appears as a 3-fold symmetric propeller-shaped supramolecule when viewed from above but when viewed from the side appears as a rectangle. Chiral assemblies such as the chiral trigonal prism CTP (Figure 8B), which has two C_3-symmetric enantiomers, present an additional level of complexity when assembled on a surface. 3D supramolecules can orient along a greater number of nonequivalent axes on a surface than is possible for 2D assemblies. Nonetheless, ordered adlayers of TBP and CTP have been formed on Au(111).

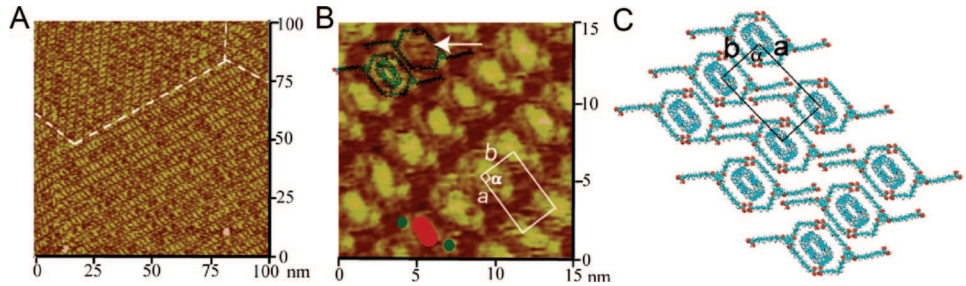

FIGURE 7. (A) Large-scale and (B) high-resolution STM images of the adlayer formed upon templation of **1** by TCDB on HOPG. Not every TCDB void is filled, as indicated by the white arrow in panel B. (C) Proposed structural model and unit cell of the mixed adlayer.

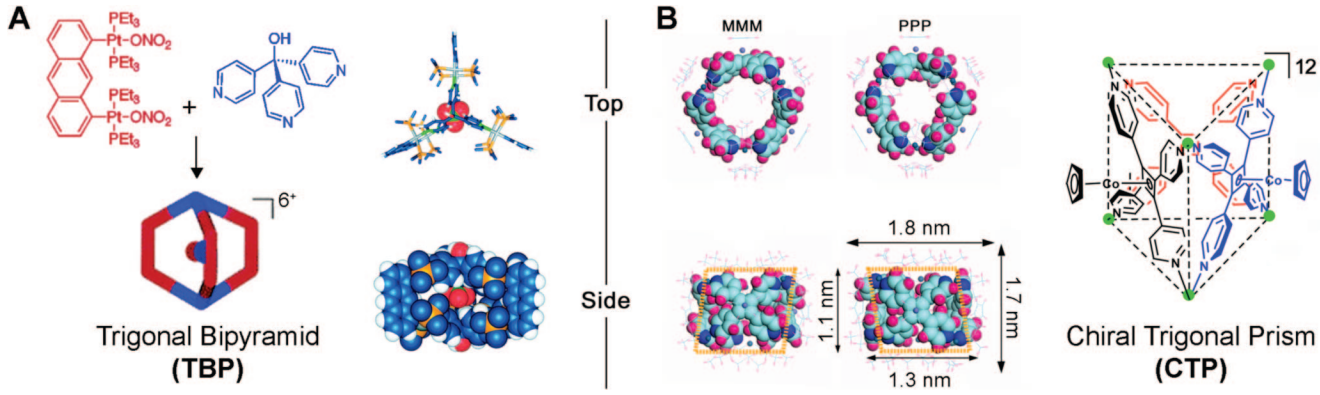

FIGURE 8. (A) Chemical structures of donor and acceptor building blocks (at left) that self-assemble to form a trigonal bipyramidal (TBP) metallacage, as well as top and side views of the TBP X-ray suprastructure, and (B) chemical structure (at right), as well as top and side views of molecular models, of the MMM and PPP enantiomers of a chiral trigonal prism (CTP).

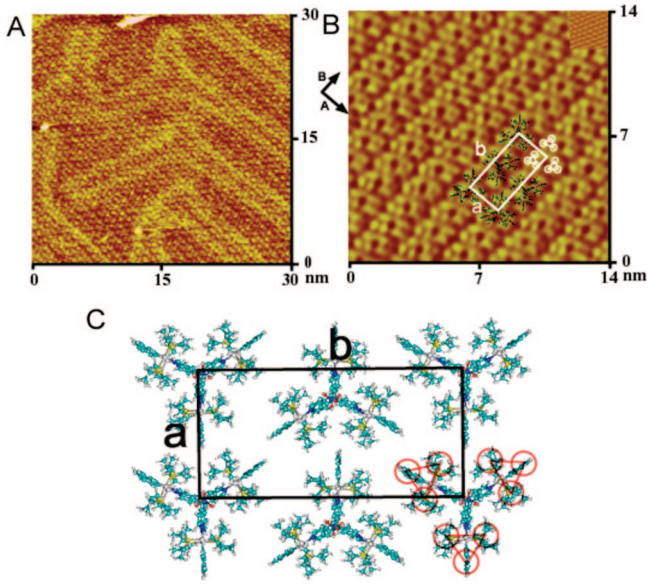

FIGURE 9. (A) Large-scale and (B) high-resolution STM images of the adlayer of TBP on Au(111) and (C) proposed structural model and unit cell of the adlayer.

Figure 9A shows a typical STM image of a well-ordered adlayer formed when a Au(111) bead is immersed in a solution of TBP.[35] The high-resolution STM image (Figure 9B) reveals the details of the cage adlayer. Within each ordered row are repeating sets of nine bright spots, each corresponding to one supramolecular TBP cage. Models of the TBP cage are superimposed (Figure 9B) on the adlayer, and white circles indicate one set of nine bright spots that makes up a single metallacage. The trigonal prisms orient along the *A* direction such that their propeller "blades" are interdigitated, while along the *A*−*B* diagonal the faces of their bis-Pt(II) anthracenyl moieties align roughly parallel. This orientation likely maximizes intermolecular van der Waals interactions and provides stability to the adlayer. It is interesting to note that similar interdigitation is not observed in the X-ray structure of the TBP, highlighting a significant difference between the 3D stacking (X-ray) and 2D ordering (adlayer) of the 3D supramolecules. A unit cell for the adlayer is outlined in Figure 9B. A model for the adlayer is proposed in Figure 9C.

A slightly more complex situation arises when chiral 3D supramolecules are assembled on a Au(111) surface. Figure 8B shows the chemical structure of the chiral trigonal prism,[50] CTP, as well as space-filling models of its helically chiral MMM and PPP enantiomers. The assembly of chiral supramolecules on solid substrates opens the possibility of forming chiral surfaces, which may find applications in heterogeneous stereoselective synthesis and catalysis. Immersion of a gold bead in a 10^{-6} M racemic mixture of the CTP in EtOH results in the formation of well-defined chiral domains.[38] A typical large-scale STM image of the adlayer of the CTP is shown in Fig-

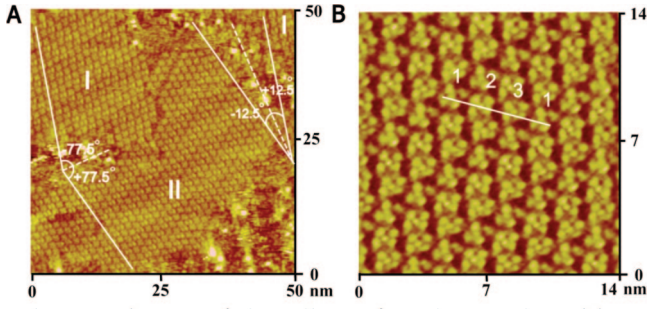

FIGURE 10. (A) Large-scale STM image of the adlayer found upon deposition of a racemic mixture of the CTP on Au(111). Separate chiral domains are indicated as I and II. (B) High-resolution STM image displaying regular rows of repeating units of a single enantiomeric domain.

ure 10A. Spontaneous symmetry breaking is observed, resulting in the formation of separated, locally chiral domains of MMM and PPP helical enantiomers, indicated as I and II. These domains cross, forming an angle of 25° ± 2°. The supramolecules lie edge-down on the gold substrate while projecting one of their three flat faces upward as in the side view shown in Figure 8B. Each trigonal prism appears as four bright spots arranged around a central bright spot, corresponding to the four pyridyl moieties and the Cp−Co center of the tetratopic donor. The orientation of the four pyridyl spots around their central Cp−Co spot distinguishes each enantiomer. The dimensions of the supramolecular entities are 1.5 nm × 1.4 nm (±0.2 nm), consistent with the side view of the CTP obtained from molecular modeling. As seen in the high-resolution STM image (Figure 10B), each row of supramolecular trigonal prisms is composed of repeating sets of three supramolecules (indicated as 1, 2, and 3) that differ slightly in their conformation with respect to the underlying Au(111) surface. It has not been possible to assign the absolute configuration of the two chiral domains because neither enantiopure surface has been prepared due to the lack of availability of the individual enantiomers.

A high-resolution image of the junction of two chiral domains is shown in Figure 11A.[38] The upper left domain has been arbitrarily assigned as being composed of MMM enantiomers with the lower right domain being composed of PPP enantiomers. The positions of the regularly repeating rows in the MMM and PPP domains are aligned differently on the underlying Au(111) surface. These differences are made more explicit in the orientations of sets of ten MMM and PPP enantiomers superimposed on their respective domains and in the rhomboidal unit cells indicated by dashed white lines in each domain. A structural model of the junction, where the relative orientations of the chiral domains have been taken from STM images and have been preserved upon transposition onto a simulated Au(111) surface, is given in Figure 11B. Single enantiomeric trigonal prisms are shown in the upper left (MMM) and right (PPP) corners, clearly displaying their mirror image relationship. An angle of 26° is formed where the two domains cross along the θ direction of the substrate. Unit cells are the same in both chiral domains. The observation of domain separation of a racemic mixture of supramolecular trigonal prisms sheds light on the process of self-assembly of chiral moieties on 2D substrates, indicating that the adsorption of a trigonal prism of one chirality likely "seeds" the adsorption of like-chirality prisms. Given that the adsorbate−substrate interactions between MMM and PPP enantiomers of the CTP are the same, these results again highlight the vital importance of intermolecular interactions, which in this example must be stronger between adsorbates of the same absolute configuration than between enantiomeric pairs.

Conclusion

Constructing and controlling supramolecular architectures that exhibit desirable structural as well as electronic, magnetic, catalytic, photonic, and other properties is a constant challenge in materials science. The results presented in this Account demonstrate that various metallosupramolecular architectures can be built under mild conditions by employing facile self-assembly methods. The supramolecules retain their chemical structures without dissociation, a necessary requirement for

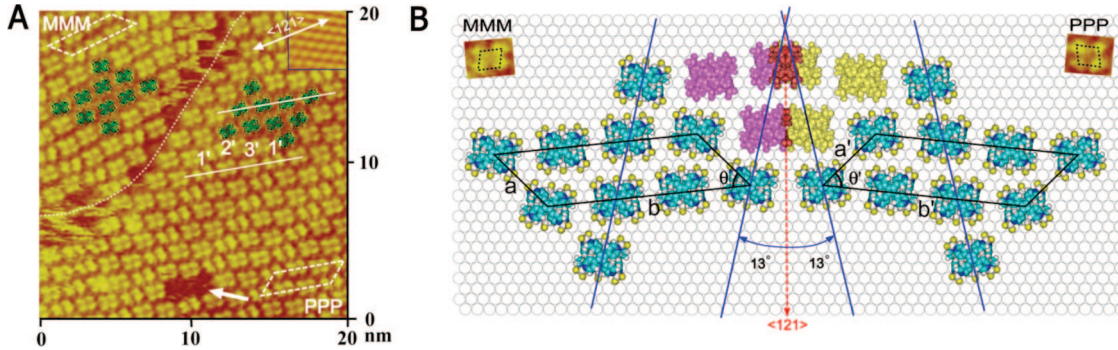

FIGURE 11. (A) High-resolution STM image and (B) proposed model of the junction of two domains of opposite chirality on Au(111).

the construction of robust materials. STM has proven to be an indispensable and powerful tool for characterizing the structural details of these supramolecular surface adlayers. The results shed new insight into the adsorption, mobility, stability, and lateral interactions that play an important role in fabricating metallosupramolecular architectures and that depend upon the chemical nature and symmetry of the substrate and the influence of substrate−molecule interactions. Ultimately, these studies contribute to the knowledge base that is a prerequisite of, and necessary for, the "bottom-up" nanofabrication of molecular devices.

It is likely that the first examples of molecular materials based upon integrating metallosupramolecules with solid supports will be those that take advantage of the reduced symmetry of a 2D surface. Metallacycles that form adlayers with their supramolecular cavities oriented parallel with the surface are well suited to be used as hosts that are capable of selectively binding a variety of guests based upon size and shape complementarity as well as noncovalent host−guest interactions. Metallosupramolecular assemblies with magnetic or electronic properties will likely benefit from surface adsorption, because orientational control can be utilized to align spins or orbitals, respectively. Heterogeneous surface catalysis may be envisioned wherein the alignment of catalytic active sites can be tailored to be selective for particular chemical transformations on the basis of metallosupramolecular adlayer structure. While there is still much to be done in order to bring these goals to fruition, thorough investigations of the preparation, observation, and control of metallosupramolecular adlayers on surfaces are an essential aid in the development of such materials.

The authors thank all of the co-workers who have contributed to this research, whose names can be found in the literature cited herein. L.J.W. thanks the National Natural Science Foundation of China (Grant Nos. 20575070, 20673121, and 20733004), National Key Project on Basic Research (Grants 2006CB806100 and 2006CB932104), and the Chinese Academy of Sciences for support. P.J.S. thanks the NIH (Grant GM-57052) and the NSF (Grants CHE-0306720 and CHE-0820955) for support. B.H.N. thanks the NIH (Grant GM-080820) for support.

BIOGRAPHICAL INFORMATION

Shan-Shan Li received her Ph.D. in Physical Chemistry from ICCAS under the supervision of Prof. Li-Jun Wan in 2008. Her research interests include the study of single molecules, the self-assembly of metal-coordinated supramolecules, and molecular monodispersion investigated with electrochemical STM. She is currently working in the State Intellectual Property Office of China.

Brian H. Northrop received his B.A. degree in Chemistry in 2001 from Middlebury College in Vermont while working with Professor J. Byers. In 2002, he joined the laboratories of Professors K. N. Houk and J. F. Stoddart in the Department of Chemistry and Biochemistry at the University of California, Los Angeles, and obtained his Ph.D. in 2006. Shortly thereafter he moved to Utah and joined the laboratory of Professor P. J. Stang as an NIH postdoctoral fellow, where he is conducting research on the self-assembly of metal−organic metallacycles and metallacages focusing on their functionalization, assembly onto surfaces, and ability to act as abiological hosts for the complexation of biologically relevant compounds.

Qun-Hui Yuan received her Ph.D. in Physical Chemistry from ICCAS under the supervision of Prof. Li-Jun Wan in 2006. Her research has centered on the structural relationship between ligands and their corresponding metal-coordinated complexes, the self-assembly of metal-coordinated complexes, and molecular chirality on two-dimensional surfaces using electrochemical STM.

Prof. Li-Jun Wan received his Ph.D. in Materials Chemistry from Tohoku University of Japan in 1996. From 1996 to 1999, he worked at the Japan Science and Technology Agency (JST), Hokkaido University, and Tohoku University conducting research in atomic/molecular structure formation, transition, and STM characterization at solid/liquid interfaces as a researcher and visiting professor. In 1999, he joined the Institute of Chemistry of Chinese Academy of Science (ICCAS) as a professor and is currently the director of ICCAS. His research areas involve molecular self-assembly, functional nanomaterials, electrochemistry, and scanning probe microscopy (SPM).

Peter J. Stang is a Distinguished Professor of Chemistry at the University of Utah, as well as the Editor of the *Journal of the American Chemical Society*. He is a member of the National Academy of Sciences and the American Academy of Arts and Sciences and a Foreign Member of the Chinese and Hungarian Academies of Sciences.

FOOTNOTES

* To whom correspondence should be addressed. E-mail addresses: wanlijun@iccas.ac.cn; stang@chem.utah.edu.

REFERENCES

1 See, for example: Kay, E. R.; Leigh, D. A.; Zerbetto, F. Synthetic Molecular Motors and Mechanical Machines. *Angew. Chem., Int. Ed.* **2007**, *46*, 72–191.

2 (a) Lathan, A. H.; Williams, M. E. Controlling Transport and Chemical Functionality of Magnetic Nanoparticles. *Acc. Chem. Res.* **2008**, *41*, 411–420. (b) Rosi, N. L.; Giljohann, D. A.; Thaxton, C. S.; Lytton-Jean, A.; Han, M. S.; Mirkin, C. A. Oligonucleotide-Modified Gold Nanoparticles for Intracellular Gene Regulation. *Science* **2006**, *312*, 1027–1030.

3 Barlow, S. M.; Raval, R. Complex Organic Molecules at Metal Surfaces: Bonding, Organization and Chirality. *Surf. Sci. Rep.* **2003**, *50*, 201–341, and references therein.

4 See, for example: van Delden, R. A.; ter Wiel, M. K. J.; Pollard, M. M.; Vicario, J.; Koumura, N.; Feringa, B. L. Undirectional Molecular Motor on a Gold Surface. *Nature* **2005**, *437*, 1337–1340.

5 Gates, B. G.; Xu, Q.; Stewart, M.; Ryan, D.; Wilson, C. G.; Whitesides, G. M. New Approaches to Nanofabrication: Molding, Printing, and Other Techniques. *Chem. Rev.* **2005**, *105*, 1171–1196.

6 (a) Gomar-Nadal, E.; Puigmarti-Luis, J.; Amabilino, D. B. Assembly of Functional Molecular Nanostructures on Surfaces. *Chem. Soc. Rev.* **2008**, *37*, 409–504. (b) Guo, L. J. Nanoimprint Lithography: Methods and Material Requirements. *Adv. Mater.* **2007**, *19*, 495–513. (c) Henzie, J.; Barton, J. E.; Stender, C. L.; Odom, T. W. Large-Area Nanoscale Patterning: Chemistry Meets Fabrication. *Acc. Chem. Res.* **2006**, *39*, 249–257.

7 Balzani, G.; Credi, A.; Venturi, M. The Bottom-Up Approach to Molecular-Level Devices and Machines. *Chem.—Eur. J.* **2002**, *8*, 5525–5532.

8 Lehn, J. M. Toward Complex Matter: Supramolecular Chemistry and Self-Organization. *Proc. Natl. Acad. Sci. U.S.A.* **2002**, *99*, 4763–4768.

9 Whitesides, G. M.; Boncheva, M. Beyond Molecules: Self-Assembly of Mesoscopic and Macroscopic Components. *Proc. Natl. Acad. Sci. U.S.A.* **2002**, *99*, 4769–4774.

10 Lehn, J. M. *Supramolecular Chemistry: Concept and Perspectives*; VCH: New York, 1995.

11 Howard, J. *Mechanics of Motor Proteins and the Cytoskeleton*; Sinauer: Sunderland, MA, 2001.

12 Kolb, D. M. Electrochemical Surface Science. *Angew. Chem., Int. Ed.* **2001**, *40*, 1162–1181.

13 De Feyter, S.; De Schryver, F. C. Self-Assembly at the Liquid/Solid Interface: STM Reveals. *J. Phys. Chem. B* **2005**, *109*, 4290–4302.

14 Gimzewski, J. K.; Joachim, C. Nanoscale Science of Single Molecules using Local Probes. *Science* **1999**, *283*, 1683–1688.

15 Barth, J. V.; Costantini, G.; Kern, K. Engineering Atomic and Molecular Nanostructures at Surfaces. *Nature* **2005**, *437*, 671–679.

16 (a) Seidel, S. R.; Stang, P. J. High Symmetry Coordination Cages via Self-Assembly. *Acc. Chem. Res.* **2002**, *35*, 972–983. (b) Leininger, S.; Olenyuk, B.; Stang, P. J. Self-Assembly of Discrete Cyclic Nanostructures Mediated by Transition Metals. *Chem. Rev.* **2000**, *100*, 853–907. (c) Stang, P. J.; Olenyuk, B. Self-Assembly, Symmetry and Molecular Architecture: Coordination as the Motif in the Rational Design of Supramolecular Metallacyclic Polygons and Polyhedra. *Acc. Chem. Res.* **1997**, *30*, 502–518. (d) Northrop, B. H.; Yang, H.-B.; Stang, P. J. Coordination-Driven Self-Assembly of Functionalized Supramolecular Metallacycles. *Chem. Commun* **2008**, 5896–5908.

17 (a) Caulder, D. L.; Raymond, K. N. Supermolecules by Design. *Acc. Chem. Res.* **1999**, *32*, 975–982. (b) Johnson, D. W.; Raymond, K. N. The Role of Guest Molecules in the Self-Assembly of Metal-Ligand Clusters. *Supramol. Chem.* **2001**, *13*, 639–659. (c) Xu, J.-D.; Raymond, K. N. Structurally Characterized Quadruple-Stranded Bisbidentate Helicates. *Angew. Chem., Int. Ed.* **2006**, *45*, 6480–6485.

18 Fujita, M.; Tominaga, M.; Hori, A.; Therrien, B. Coordination Assemblies from a Pd(II)-Cornered Square Complex. *Acc. Chem. Res.* **2005**, *38*, 369–378.

19 (a) Holliday, B. J.; Mirkin, C. A. Strategies for the Construction of Supramolecular Compounds through Coordination Chemistry. *Angew. Chem., Int. Ed.* **2001**, *40*, 2022–2043. (b) Oliveri, C. G.; Gianneschi, N. C.; Nguyen, S. T.; Mirkin, C. A.; Stern, C. L.; Wawrzak, Z.; Pink, M. Supramolecular Allosteric Cofacial Porphyrin Complexes. *J. Am. Chem. Soc.* **2006**, *128*, 16286–16296.

20 Lehn, J. M. From Supramolecular Chemistry Towards Constitutional Dynamic Chemistry and Adaptive Chemistry. *Chem. Soc. Rev.* **2007**, *36*, 151–160.

21 Lee, S. J.; Hupp, J. T. Porphyrin-Containing Molecular Squares: Design and Applications. *Coord. Chem. Rev.* **2006**, *250*, 1710–1723.

22 See, for example: Thanasekaran, P.; Wu, J.-Y.; Manimaran, B.; Rajendran, T.; Chang, I.-J.; Rajagopal, S.; Lee, G.-H.; Peng, S.-M.; Lu, K.-L. Aggregate of Alkoxyl-Bridged Re(I)-Rectangles as a Probe for Photolulminescence Quenching. *J. Phys. Chem. A* **2007**, *111*, 10953–10960.

23 Resendiz, M. J. E.; Noveron, J. C.; Disteldorf, H.; Fischer, S.; Stang, P. J. A Self-Assembled Supramolecular Optical Sensor for Ni(II), Cd(II), and Cr(III). *Org. Lett.* **2004**, *6*, 651–653.

24 Ziegler, M.; Davis, A. V.; Johnson, D. W.; Raymond, K. N. Supramolecular Chirality: A Reporter of Structural Memory. *Angew. Chem., Int. Ed.* **2003**, *42*, 665–668.

25 (a) Williams, M. E.; Benkstein, K. D.; Abel, C.; Dinolfo, P. H.; Hupp, J. T. Shape-Selective Transport through Rectangle-Based Molecular Materials: Thin-Film Scanning Electrochemical Microscopy Studies. *Proc. Natl. Acad. Sci. U.S.A.* **2002**, *99*, 5171–5177.

26 Wan, L. J. Fabricating and Controlling Molecular Self-Organization at Solid Surfaces: Studies by Scanning Tunneling Microscopy. *Acc. Chem. Res.* **2006**, *39*, 334–342.

27 Chiang, S. Scanning Tunneling Microscopy Imaging of Small Adsorbed Molecules on Metal Surfaces in an Ultrahigh Vacuum Environment. *Chem. Rev.* **1997**, *97*, 1083–1096.

28 Itaya, K. In Situ Scanning Tunneling Microscopy in Electrolyte Solutions. *Prog. Surf. Sci.* **1998**, *58*, 121–247.

29 Wan, L. J.; Noda, H.; Wang, C.; Bai, C. L.; Osawa, M. Controlled Orientation of Individual Molecules by Electrode Potentials. *ChemPhysChem* **2001**, *2*, 617–619.

30 Wang, D.; Wan, L. J. Electrochemical Scanning Tunneling Microscopy: Adlayer Structure and Reaction at Solid/Liquid Interface. *J. Phys. Chem. C* **2007**, *111*, 16109–16130.

31 Semenov, A.; Spatz, J. P.; Moller, M.; Lehn, J. M.; Sell, B.; Schubert, D.; Weidl, C. H.; Schubert, U. S. Controlled Arrangement of Supramolecular Metal Coordination Arrays on Surfaces. *Angew. Chem., Int. Ed.* **1999**, *38*, 2547–2550.

32 Ziener, U.; Lehn, J. M.; Mourran, A.; Moller, M. Supramolecular Assemblies of a Bis(terpyridine) Ligand and of its [2 × 2] Grid-Type Zn-II and Co-II Complexes on Highly Ordered Pyrolytic Graphite. *Chem.—Eur. J.* **2002**, *8*, 951–957.

33 Kurth, D. G.; Severin, N.; Rabe, J. P. Perfectly Straight Nanostructures of Metallosupramolecular Coordination-Polyelectrolyte Amphiphile Complexes on Graphite. *Angew. Chem., Int. Ed.* **2002**, *41*, 3681–3683.

34 (a) Safarowsky, C.; Merz, L.; Rang, A.; Broekmann, P.; Hermann, B. A.; Schalley, C. A. Second-Order Templation: Ordered Deposition of Supramolecular Squares on a Chlorine-Covered Cu(100) Surface. *Angew. Chem., Int. Ed.* **2004**, *43*, 1291–1294. (b) Jeong, K. S.; Kim, S. Y.; Shin, U.-S.; Kogej, M.; Hai, N. T. M.; Broekmann, P.; Jeong, N.; Kirchner, B.; Reiher, M.; Schalley, C. A. Synthesis of Chiral Self-Assembling Rhombs and Their Characterization in Solution, in the Gas Phase, and at the Liquid-Solid Interface. *J. Am. Chem. Soc.* **2005**, *127*, 17672–17685.

35 Yuan, Q. H.; Wan, L. J.; Jude, H.; Stang, P. J. Self-Organization of a Self-Assembled Supramolecular Rectangle, Square, and Three-Dimensional Cage on Au(111) Surfaces. *J. Am. Chem. Soc.* **2005**, *127*, 16279–16286.

36 Gong, J. R.; Wan, L. J.; Yuan, Q. H.; Bai, C. L.; Jude, H.; Stang, P. J. Mesoscopic Self-Organization of a Self-Assembled Supramolecular Rectangle on Highly Oriented Pyrolytic Graphite and Au(111) Surfaces. *Proc. Natl. Acad. Sci. U.S.A.* **2005**, *102*, 971–974.

37 Li, S. S.; Yan, H. J.; Wan, L. J.; Yang, H. B.; Northrop, B. H.; Stang, P. J. Control of Supramolecular Rectangle Self-Assembly with a Molecular Template. *J. Am. Chem. Soc.* **2007**, *129*, 9268–9269.

38 Yuan, Q.-H.; Yan, C.-J.; Yan, J.-H.; Wan, L.-J.; Northrop, B. H.; Jude, H.; Stang, P. J. An STM Investigation of a Supramolecular Self-Assembled 3-Dimensional Chiral Prism on a Au(111) Surface. *J. Am. Chem. Soc.* **2008**, *130*, 8878–8879.

39 Yuan, Q.-H.; Wan, L.-J. Structural Comparison of Self-Organized Adlayers of Ligands and their Metal-Coordinated Complexes on a Au(111) Surface: An STM Study. *Chem.—Eur. J.* **2006**, *12*, 2808–2814.

40 (a) Chen, X.; Lenhert, S.; Hirtz, M.; Lu, N.; Fuchs, H.; Chi, L. Langmuir—Blodgett Patterning: A Bottom-Up Way to Build Mesostructures over Large Areas. *Acc. Chem. Res.* **2007**, *40*, 393–401.

41 Xu, X. M.; Zhong, H. P.; Zhang, H. M.; Mo, Y. R.; Xie, Z. X.; Long, L. S.; Zheng, L. S.; Mao, B. W. Ordered Silver Adlayer Formation by Surface-Induced Dissociation of a Coordination Complex Precursor on Au(111) and Au(100) Surfaces. *Chem. Phys. Lett.* **2004**, *386*, 254–258.

42 Ruben, M.; Rojo, J.; Romero-Salguero, F. J.; Uppadine, L. H.; Lehn, J. M. Grid-Type Metal Ion Architectures: Functional Metallosupramolecular Arrays. *Angew. Chem., Int. Ed.* **2004**, *43*, 3644–3662.

43 Schalley, C. A.; Lutzen, A.; Albrecht, M. Approaching Supramolecular Functionality. *Chem.—Eur. J.* **2004**, *10*, 1072–1080.

44 See, for example: Braunschweig, A. B.; Northrop, B. H.; Stoddart, J. F. Structural Control at the Organic-Solid Interface. *J. Mater. Chem.* **2006**, *16*, 32–44.

45 Kuehl, C. J.; Huang, S. D.; Stang, P. J. Self-Assembly with Postmodification: Kinetically Stabilized Metalla-Supramolecular Rectangles. *J. Am. Chem. Soc.* **2001**, *123*, 9634–9641.

46 Stang, P. J.; Cao, D. H.; Saito, S.; Arif, A. M. Self-Assembly of Cationic, Tetranuclear, Pt(II) and Pd(II) Macrocyclic Squares. X-Ray Crystal-Structure of $[Pt^{2+}(dppp)(4,4'\text{-bipyridyl}) \cdot 2^{-}OSO_2CF_3]_4$. *J. Am. Chem. Soc.* **1995**, *117*, 6273–6283.

47 Lu, J.; Lei, S. B.; Zeng, Q. D.; Kang, S. Z.; Wang, C.; Wan, L. J.; Bai, C. L. Template-Induced Inclusion Structures with Copper(II) Phthalocyanine and Coronene as Guests in Two-Dimensional Hydrogen-Bonded Host Networks. *J. Phys. Chem. B* **2004**, *108*, 5161–5165.

48 Lu, J.; Zeng, Q. D.; Wang, C.; Zheng, Q. Y.; Wan, L. J.; Bai, C. L. Self-Assembled Two-Dimensional Hexagonal Networks. *J. Mater. Chem.* **2002**, *12*, 2856–2858.

49 Kuehl, C. J.; Kryschenko, Y. K.; Radhakrishnan, U.; Seidel, S. R.; Huang, S. D.; Stang, P. J. Self-Assembly of Nanoscopic Coordination Cages of D_{3h} Symmetry. *Proc. Natl. Acad. Sci. U.S.A.* **2002**, *99*, 4932–4936.

50 Caskey, D. C.; Yamamoto, T.; Addicott, C.; Shoemaker, R. K.; Vacek, J.; Horinek, D.; Hawkridge, A. M.; Muddiman, D. C.; Kottas, G.; Michl, J.; Stang, P. J. Coordination-Driven Face-Directed Self-Assembly of Trigonal Prisms. Face-Based Conformational Chirality. *J. Am. Chem. Soc.* **2008**, *130*, 7620–7628.